

Continuous-discrete smoothing of diffusions

Frank van der Meulen and Moritz Schauer

Delft Institute of Applied Mathematics (DIAM)
Delft University of Technology
 Mekelweg 4
 2628 CD Delft
 The Netherlands
 e-mail: f.h.vandermeulen@tudelft.nl

Mathematical Institute
Leiden University
 P.O. Box 9512
 2300 RA Leiden
 The Netherlands
 e-mail: m.r.schauer@math.leidenuniv.nl

Abstract Suppose X is a multivariate diffusion process that is observed discretely in time. At each observation time, a linear transformation of the state of the process is observed with additive noise. The smoothing problem consists of recovering the path of the process, consistent with the observations. We derive a novel Markov Chain Monte Carlo algorithm to sample from the exact smoothing distribution. Key to this is an extension of the linear guided proposals introduced in [Schauer et al. \(2017\)](#). We illustrate the efficiency of our method on both the Lorenz system and a partially observed integrated diffusion model.

Keywords: diffusion bridge, filtering, guided proposal, integrated diffusion, Lorenz system, partial observations, preconditioned Crank-Nicholson

Primary 60J60, 65C05; secondary 62F15.

1. Introduction

Suppose X is a diffusion process with dynamics governed by the stochastic differential equation (SDE)

$$dX_t = b(t, X_t) dt + \sigma(t, X_t) dW_t. \quad (1.1)$$

Here, $b: \mathbb{R}_+ \times \mathbb{R}^d \rightarrow \mathbb{R}^d$ and $\sigma: \mathbb{R}_+ \times \mathbb{R}^d \rightarrow \mathbb{R}^{d \times d'}$ are the drift and dispersion coefficient respectively. The process W is a vector valued process in $\mathbb{R}^{d'}$ consisting of independent Brownian motions. It is assumed that the required conditions for existence of a strong solution are satisfied (Cf. [Karatzas and Shreve \(1991\)](#)). We assume that we observe the process partially at a finite set of observation times with additive noise. More precisely, we assume observation times $0 = t_0 < t_1 < \dots < t_n$ and observations

$$V_i = L_i X_{t_i} + \eta_i, \quad i = 0, \dots, n, \quad (1.2)$$

where L_i is a $m_i \times d$ -matrix and $\eta_i \sim N_{m_i}(0, \Sigma_i)$ are independent random variables, independent of the diffusion process X .

Let D denote the set of observations, i.e. $D = \{V_i, i = 0, \dots, n\}$. We assume that b , σ and $\{\Sigma_i, i = 0, \dots, n\}$ are known, so that there is no need for parameter estimation. Instead, we focus on the *smoothing problem*, which consists of reconstructing the path $\{X_t, t \in [0, T]\}$ based on D . The problem of recovering unobserved states in a dynamical system has been studied by many authors in case of either “discrete dynamics–discrete observations” or

“continuous dynamics–continuous observations”. Here, we deal with the *hybrid* case where we assume “continuous dynamics-discrete observations”.

1.1. Related work

If the diffusion process is fully observed at all times $\{t_i, 0 \leq i \leq n\}$ without noise, then the smoothing problem reduces to the sampling of n independent diffusion bridges. This problem has attracted considerable attention over the past two decades, see for instance [Eraker \(2001\)](#), [Elerian et al. \(2001\)](#), [Durham and Gallant \(2002\)](#), [Clark \(1990\)](#), [Bladt et al. \(2016\)](#), [Beskos et al. \(2008\)](#), [Hairer et al. \(2009\)](#), [Bayer and Schoenmakers \(2013\)](#), [Lin et al. \(2010\)](#), [Beskos et al. \(2006\)](#), [Delyon and Hu \(2006\)](#), [Lindström \(2012\)](#), [Schauer et al. \(2017\)](#) and [Whitaker et al. \(2017\)](#). In the general case however, the connecting bridges cannot be sampled independently between adjacent observation times. In fact, at time $t \in (t_{i-1}, t_i)$ the process X , conditioned on D , depends on all future conditionings V_i, \dots, V_n . To resolve this problem, subsequent simulation of bridges on overlapping intervals has been proposed by [Golightly and Wilkinson \(2008\)](#), [Fuchs \(2013\)](#) and [van der Meulen and Schauer \(2017b\)](#).

[Särkkä and Sottinen \(2008\)](#) considered *filtering* (instead of smoothing) of diffusions under the assumption that the dispersion coefficient is only allowed to depend on time. If the diffusion can be transformed to unit diffusion coefficient, then filtering can also be accomplished using the exact algorithm for simulation of diffusions, as introduced by [Beskos and Roberts \(2005\)](#). This algorithm forms the basis for the methods presented in [Fearnhead et al. \(2008\)](#) and [Olsson and Ströjby \(2011\)](#). Various solutions to the filtering and smoothing problem are further discussed in [Särkkä and Sarmavuori \(2013\)](#). Key to the proposed algorithms therein is the assumption that the distribution of X_t , conditional on the data D can be approximated by the normal distribution.

1.2. Approach

For $i < j$ set $X_{(i:j)} = \{X_t, t \in (t_i, t_j)\}$. In [van der Meulen and Schauer \(2017b\)](#) the following Markov Chain Monte Carlo (MCMC) scheme was proposed for smoothing:

1. Initialise $X_{(0:n)}$.
2. For $i = 1, \dots, n/2$, sample bridges $X_{(2i-2:2i)}$, conditional on $X_{2i-2}, V_{2i-1}, X_{2i}$.
3. For $i = 1, \dots, n/2 - 1$, sample bridges $X_{(2i-1:2i+1)}$, conditional on X_{2i-1}, V_{2i} and X_{2i+1} .
Sample $X_{(0:1)}$ conditional on V_0 and X_1 . Sample $X_{(n-1:n)}$ conditional on V_n and X_{n-1} .

(assuming n is even; the case n being odd can be dealt with similarly). In this paper we build upon this work and show that it is computationally just as easy to work with larger blocks of overlapping intervals. The most extreme case consists of a single block that consists of the complete path $(X_t, t \in [0, t_n])$. Assume that X admits smooth transition densities p . That is, for $s < \tau$, $P^{(s,x)}(X_\tau \in dy) = p(s, x; \tau, y) dy$. The starting point we take is theorem 2.3.4 from [Marchand \(2012\)](#). For this result the theory of initial enlargement of filtrations is used to derive the SDE for the process X at time $t \in (t_{i-1}, t_i)$, conditioned on V_i, \dots, V_n while assuming that $\eta_i \equiv 0$ for all i . From this result it is easily derived that when there is nonzero noise on the observations, the SDE for the conditioned process is given by

$$dX_t^* = b(t, X_t^*) dt + a(t, X_t^*) r(t, X_t^*) dt + \sigma(t, X_t^*) dW_t, \quad X_{t_{i-1}}^* = x_{t_{i-1}}.$$

Here $a(t, x) = \sigma(t, x)\sigma(t, x)'$. Furthermore, $r(t, x) = D \log \rho(t, x)$ (the column vector containing all partial derivatives of $\log \rho(t, x)$ with respect to x), where ρ is defined by

$$\rho(t, x) = \int p(t, x; t_i, \xi_i) \prod_{j=i}^n p(t_j, \xi_j; t_{j+1}, \xi_{j+1}) q_j(v_j - L_j \xi_j) d\xi_i \cdots d\xi_n, \quad (1.3)$$

with q_j denoting the density of the $N(0, \Sigma_j)$ distribution. Since p is only known in closed form in very specific instances, ρ is intractable and hence it is not possible to simulate directly from X^* . The key idea in [Schauer et al. \(2017\)](#), which addressed the simpler problem of diffusion bridge simulation, is to replace the unknown transition density p by a tractable transition density \tilde{p} of another diffusion process. Next, one simulates from the process which satisfies the SDE

$$dX_t^\circ = b(t, X_t^\circ) dt + a(t, X_t^\circ) \tilde{r}(t, X_t^\circ) dt + \sigma(t, X_t^\circ) dW_t, \quad X_{t_{i-1}}^\circ = x_{t_{i-1}}, \quad (1.4)$$

where $\tilde{r}(t, x) = D \log \tilde{\rho}(t, x)$ and $\tilde{\rho}(t, x)$ is defined as $\rho(t, x)$ with the transition densities \tilde{p} replacing p . If the laws of the processes X° and X^* are absolutely continuous, then one can simulate from X° instead of X^* and correct for the discrepancy between these processes by the Radon-Nikodym derivative of their induces laws on $C([0, t_n])$. As the SDE for X° is obtained from the SDE for X by superimposing a guiding term, these are called *guided proposals* (“proposal” as the process X° is actually used as a proposal in a Metropolis-Hastings step).

While this approach is conceptually clear, it is far from straightforward how to evaluate \tilde{r} and the Radon-Nikodym derivative efficiently. It is the purpose of this paper to show how this can be done in case \tilde{p} is the transition density of a linear process \tilde{X} , i.e. a process satisfying the SDE

$$d\tilde{X}_t = \left(\tilde{\beta}(t) + \tilde{B}(t) \tilde{X}_t \right) dt + \tilde{\sigma}(t) dW_t. \quad (1.5)$$

Intuitively, the drift and dispersion of \tilde{X} should be chosen such that \tilde{X} is similar to X in areas visited by the true conditional process. With this choice it turns out that the computations consist of

- solving 2 systems of ordinary differential equations backwards in time;
- iteratively simulating forward X° and computing the Radon-Nikodym derivative between the laws of X^* and X°

Here, the first step only needs to be executed once and is akin to the updating equations in Kalman filtering. In the second step we use the Metropolis-Hastings algorithm in which we update the driving Wiener increments of the smoothed path using a preconditioned Crank-Nicolson scheme (Cf. [Cotter et al. \(2013\)](#) and [Beskos et al. \(2008\)](#)). These rather simple steps, together with its general applicability, are appealing in our opinion. We illustrate the effectiveness of our approach in a couple of benchmark examples.

We believe the proposed algorithm has a number of attractive properties:

1. It is a computationally simple algorithm that provides a unified approach to smoothing of both hypo-elliptic and uniformly elliptic diffusions.
2. It allows for taking into account nonlinearities in the drift efficiently.
3. It allows the dispersion coefficient to be state-dependent.
4. The algorithm targets the exact smoothing distribution and does not use the Normal approximation in its derivation.

Regarding the final point, we derive our algorithm in continuous time, but ultimately in any implementation the SDE for X° needs to be discretised. However, choosing the mesh-width

for the discretization can be controlled by the user. We additionally give an adaptive MCMC scheme for tuning \tilde{B} , $\tilde{\beta}$ and $\tilde{\sigma}$. Although we present our work in the context of smoothing, we believe our results also offer great potential for filtering problems and fixed-lag smoothing. In case (static) parameters appear in the drift and/or dispersion coefficient, these can either be estimated using a data-augmentation approach or an approach where a joint update on these parameters and the smoothed path is used. Compared to [Särkkä and Sarmavuori \(2013\)](#), we do not need approximations using the normal distribution. However, our approach is presently restricted to observations scheme (1.2), whereas [Särkkä and Sarmavuori \(2013\)](#) allow for nonlinearities in the observation equation.

1.3. Outline

In section 2 we consider the case of two future conditionings. Here we first review key concepts from [Schauer et al. \(2017\)](#) and [van der Meulen and Schauer \(2017b\)](#) in subsection 2.1. The backward differential equations that are key to the derived algorithm are subsequently derived in subsections 2.2 and 2.3. In section 3 we show how the general case of n future conditionings can be obtained from the results for $n = 2$. We provide an intuitive explanation for the derived formulas in section 4. Next, the backward differential equations are used in the definition of our smoothing algorithm in section 5. In subsection 5.1 we comment on the choice of the auxiliary process \tilde{X} . We conclude with numerical examples in section 6. The appendix contains a few implementational details.

2. Two future conditionings

In this section we consider the smoothing problem where $n = 2$ and X_0 is fully observed. Hence, assume observations at times 0, S and T (where $0 < S < T$) with $V_0 = X_0$, $V_S = L_S X_S + \eta_S$ and $V_T = L_T X_T + \eta_T$. Suppose Σ_S and Σ_T are the covariance matrices of η_S and η_T respectively. Assume $L_S \in \mathbb{R}^{m_S \times d}$ and $L_T \in \mathbb{R}^{m_T \times d}$. The process X , conditioned on (V_S, V_T) satisfies the SDE

$$dX_t^* = b(t, X_t^*) dt + a(t, X_t^*) r(t, X_t^*) dt + \sigma(t, X_t^*) dW_t, \quad X_0^* = x_0,$$

where $r(t, x) = D \log \rho(t, x)$. Here, $r(t, x)$ is obtained from (1.3)

$$\rho(t, x) = \begin{cases} \int p(t, x; S, \xi_S) p(S, \xi_S; T, \xi_T) \varphi(v_S - L_S \xi_S; \Sigma_S) \varphi(v_T - L_T \xi_T; \Sigma_T) d\xi_S d\xi_T & t \in [0, S] \\ \int p(t, x; T, \xi_T) \varphi(v_T - L_T \xi_T; \Sigma_T) d\xi_T & t \in (S, T] \end{cases},$$

where $\varphi(y; \Sigma)$ denotes the density of the $N(0, \Sigma)$ distribution, evaluated at y .

2.1. Recap guided proposals

Here we recap the fundamentals from [Schauer et al. \(2017\)](#) and [van der Meulen and Schauer \(2017b\)](#), applied to the setting of two future conditionings. The guided proposal X° is defined as in (1.4):

$$dX_t^\circ = b(t, X_t^\circ) dt + a(t, X_t^\circ) \tilde{r}(t, X_t^\circ) dt + \sigma(t, X_t^\circ) dW_t, \quad X_0^\circ = x_0,$$

where $\tilde{r}(t, x) = D \log \tilde{\rho}(t, x)$ and $\tilde{\rho}(t, x)$ is defined as $\rho(t, x)$, but with p replaced by the transition densities \tilde{p} of the linear process in (1.5). Throughout, we adopt the following assumption.

Assumption 2.1. There exists a strong solution for the SDE for X° , as defined in (1.4) (in the sense of definition V.10.9 of Rogers and Williams (2000)) jointly measurable with respect to starting point and path $W \in \mathbb{R}^d$.

Deviations of X° from X^\star can be corrected by their likelihood ratio, provided the laws of X° and X^\star (considered as Borel measures on $C[0, T]$) are absolutely continuous. We denote the laws of X^\star and X° viewed as measures on the space $C([0, T], \mathbb{R}^d)$ of continuous functions from $[0, T]$ to \mathbb{R}^d equipped with its Borel- σ -algebra by \mathbb{P}^\star and \mathbb{P}° respectively. By theorem 3.3 in van der Meulen and Schauer (2017b), under boundedness and smoothness assumptions on the drift coefficient b and dispersion coefficient σ , \mathbb{P}^\star is absolutely continuous with respect to \mathbb{P}° and

$$\frac{d\mathbb{P}^\star}{d\mathbb{P}^\circ}(X^\circ) = \frac{\tilde{\rho}(0, x_0)}{\rho(0, x_0)} \Psi(X^\circ), \quad (2.1)$$

where

$$\Psi(X^\circ) = \exp \left(\int_0^T G(s, X_s^\circ) ds \right). \quad (2.2)$$

Here

$$\begin{aligned} G(s, x) &= (b(s, x) - \tilde{b}(s, x))' \tilde{r}(s, x) \\ &\quad - \frac{1}{2} \text{tr} \left([a(s, x) - \tilde{a}(s)] \left[\tilde{H}(s) - \tilde{r}(s, x) \tilde{r}(s, x)' \right] \right), \end{aligned} \quad (2.3)$$

with $\tilde{a}(s) = \tilde{\sigma}(s) \tilde{\sigma}(s)'$ and

$$\tilde{H}(s) = -D^2 \log \tilde{\rho}(s, x)$$

(it turns out that \tilde{H} does not depend on x). Here $D_{ij}^2 f(x) = \partial^2 f(x) / (\partial x_i \partial x_j)$. We conclude that computing X° and the Radon-Nikodym derivative requires evaluation of both $\tilde{r}(s, x)$ and $\tilde{H}(s)$. As we will derive in section 2.3 the crux to their efficient computation is the existence of a process $\nu(s)$ such that $\tilde{r}(s, x) = \tilde{H}(s)(\nu(s) - x)$ in case \tilde{X} is a linear process.

2.1.1. Small noise on the observations

We assume nonzero noise on the observations. If there would be no noise, then absolute continuity of \mathbb{P}^\star with respect to \mathbb{P}° is not automatic. Suppose for example that the diffusion is elliptic, i.e. for all $(t, x) \in \mathbb{R} \times \mathbb{R}^d$ and $y \in \mathbb{R}^d$ there exists an $\varepsilon > 0$ such that $y' a(t, x) y \geq \varepsilon \|y\|^2$. In case $L_T = I$ and $\Sigma_T = 0$ (the diffusion is fully observed at time T without noise), then absolute continuity requires \tilde{a} to be chosen such that the relation $\tilde{a}(T) = a(T, x_T)$ is satisfied (Cf. theorem 1 Schauer et al. (2017)). For the hypo-elliptic case, no results have appeared in the literature yet and this is part of ongoing research.

2.2. Differential equations for evaluating \tilde{r} and \tilde{H}

For evaluating the guiding term and the likelihood ratio tractable expressions for \tilde{r} and \tilde{H} are needed. In this section we derive these expressions. To this end, define Φ to be the solution to

$$d\Phi(t) = \tilde{B}(t)\Phi(t) dt, \quad \Phi(0) = I$$

and set $\Phi(t, s) = \Phi(t)\Phi(s)^{-1}$. Define

$$\Upsilon(t) = \begin{cases} \text{Cov} \left(\begin{bmatrix} \eta'_S \\ \eta'_T \end{bmatrix} \right)' = \begin{bmatrix} \Sigma_S & 0_{m_S \times m_T} \\ 0_{m_T \times m_S} & \Sigma_T \end{bmatrix} & t \in [0, S] \\ \text{Cov}(\eta_T) = \Sigma_T & t \in (S, T] \end{cases},$$

$$\tilde{L}(t) = \begin{cases} \begin{bmatrix} L_S \Phi(S, t) \mathbf{1}_{[0, S]}(t) \\ L_T \Phi(T, t) \end{bmatrix} & t \in [0, S] \\ L_T \Phi(T, t) & t \in (S, T] \end{cases} \quad (2.4)$$

and

$$\mu(t) = \int_t^T \tilde{L}(\tau) \tilde{\beta}(\tau) d\tau, \quad t \in [0, T].$$

Note that $\mu(t) \in \mathbb{R}^{m_T}$ for $t \in (S, T]$, while $\mu(t) \in \mathbb{R}^{m_S + m_T}$ when $t \in [0, S]$. Finally, let x_{obs} be defined by

$$x_{\text{obs}}(t) = \begin{cases} \begin{bmatrix} v'_S & v'_T \end{bmatrix}' & t \in [0, S] \\ v_T & t \in (S, T] \end{cases}.$$

Note the similar structure for $\Upsilon(t)$, $\tilde{L}(t)$ and $x_{\text{obs}}(t)$ when t is either in $[0, S]$ or $(S, T]$. Throughout we assume

Assumption 2.2. For $t \in [0, T]$

$$\tilde{M}(t) = \left(\int_t^T \tilde{L}(\tau) \tilde{a}(\tau) \tilde{L}(\tau)' d\tau + \Upsilon(t) \right)^{-1}.$$

exists.

The following theorem expresses both \tilde{r} and \tilde{H} in terms of these quantities.

Theorem 2.3. If assumption 2.2 holds then for all $t \in [0, T]$,

$$\tilde{H}(t) = \tilde{L}(t)' \tilde{M}(t) \tilde{L}(t) \quad (2.5)$$

$$\tilde{r}(t, x) = \tilde{L}(t)' \tilde{M}(t) \left(x_{\text{obs}}(t) - \mu(t) - \tilde{L}(t)x \right). \quad (2.6)$$

Proof. The expressions for $t \in [0, S]$ follow from extending lemma 2.5 in [van der Meulen and Schauer \(2017b\)](#) to the case where not necessarily $\Sigma_T = 0$ and $L_T = I$. The expressions for $t \in (S, T]$ follow from equation (4.1) in [van der Meulen and Schauer \(2017b\)](#). \square

For all $t \in [0, T]$ and $x \in \mathbb{R}^d$, $\tilde{r}(t, x) \in \mathbb{R}^d$ and $\tilde{H}(t) \in \mathbb{R}^{d \times d}$. However, the dimensions of $\tilde{L}(t)$, $\tilde{M}(t)$, $\mu(t)$ and $x_{\text{obs}}(t)$ depend on whether $t \in [0, S]$ or $t \in (S, T]$. Clearly, on $[0, S]$, where we have to take into account two future conditionings, the matrices become bigger. As an example, $\tilde{M}(t)$ is of dimension $(m_S + m_T) \times (m_S + m_T)$ if $t \in [0, S]$, but of dimension $m_T \times m_T$ for $t \in (S, T]$.

Define

$$\tilde{M}^\dagger(t) = \tilde{M}(t)^{-1}.$$

Note that $\tilde{M}^\dagger(t)$ is always well defined because of assumption 2.2. Evaluation of $\tilde{r}(t, x)$ and $\tilde{H}(t)$ appears numerically cumbersome, in particular due to the inverse appearing in the definition of \tilde{M} . However, the following lemma shows that these quantities can be computed by solving three backward differential equations.

Lemma 2.4. For $t \in (S, T]$

$$d\tilde{L}(t) = -\tilde{L}(t)\tilde{B}(t) dt, \quad \tilde{L}(T) = L_T \quad (2.7)$$

$$d\tilde{M}^\dagger(t) = -\tilde{L}(t)\tilde{a}(t)\tilde{L}(t)' dt, \quad \tilde{M}^\dagger(T) = \Sigma_T \quad (2.8)$$

$$d\mu(t) = -\tilde{L}(t)\tilde{\beta}(t) dt, \quad \mu(T) = 0. \quad (2.9)$$

For $t \in [0, S]$ these equations hold as well, with

$$\tilde{L}(S) = \begin{bmatrix} 0_{m_S \times d} \\ \tilde{L}(S+) \end{bmatrix}, \quad \tilde{M}^\dagger(S) = \begin{bmatrix} \Sigma_S & 0_{m_S \times m_T} \\ 0_{m_T \times m_S} & \tilde{M}^\dagger(S+) \end{bmatrix}, \quad \mu(S) = \begin{bmatrix} 0_{m_S \times d} \\ \mu(S+) \end{bmatrix}. \quad (2.10)$$

Proof. These equations follow directly from their definitions upon differentiation. The relations in (2.10) can be verified by evaluating $\tilde{L}(t)$ for both $t = S$ and $t = S+$ (and similarly for $\tilde{M}^\dagger(t)$ and $\mu(t)$). \square

Therefore, we first solve the backward differential equation for $\tilde{L}(t)$ on $(S, T]$, use (2.10) to obtain \tilde{S} , and next solve backwards the differential equation on $[0, S]$. Then the equations for $\tilde{M}^\dagger(t)$ and $\mu(t)$ can be solved in the same way.

Remark 2.5. The value of theorem 2.3 lies in recognition of the structure on both \tilde{H} and \tilde{r} , something which was not noticed in [van der Meulen and Schauer \(2017b\)](#). The theorem shows that both quantities can be written in a unified way on both $[0, S]$ and $(S, T]$. The key to this is the proper definition of \tilde{L} (including the indicator).

Remark 2.6. Suppose $L_T = I$ and $\Sigma_T = 0$. For $t \in (S, T]$ we have that $\tilde{M}(t)$ exists if and only if $\int_t^T \Phi(T, \tau)\tilde{a}(\tau)\Phi(T, \tau)' d\tau$ is invertible. This matrix is the controllability Grammian. Systems theory provides sufficient conditions for controllability. In case $\tilde{a}(t)$ is not invertible, then $\tilde{M}(t)$ exists if and only if the pair of functions $(\tilde{B}, \tilde{\sigma})$ is controllable on $[t, T]$ for any $t \in [0, T)$ (Cf. section 5.6 in [Karatzas and Shreve \(1991\)](#)).

Remark 2.7. Suppose $L_S = I$ and $\Sigma_S = 0$. This corresponds to the case where the diffusion is fully observed at time S without noise. By the Markov property, the pulling term should only depend on v_S (which is then in fact x_S) and not on v_T . To verify this, first note that we can write

$$\tilde{M}^\dagger(t) = \begin{bmatrix} A & C \\ C' & D \end{bmatrix},$$

where for $t \in [0, S)$

$$\begin{aligned} A &= \int_t^S L_S \Phi(S, \tau) \tilde{a}(\tau) \Phi(S, \tau)' d\tau \\ C &= \int_t^S L_S \Phi(S, \tau) \tilde{a}(\tau) \Phi(T, \tau)' L_T' d\tau = A \Phi(T, S)' L_T' \\ D &= \int_t^T L_T \Phi(T, \tau) \tilde{a}(\tau) \Phi(T, \tau)' L_T' d\tau. \end{aligned}$$

Now assume $L_S = I$ and A is invertible. Then we have

$$\tilde{L}(t) = \begin{bmatrix} L_S \\ L_T \Phi(T, S) \end{bmatrix} \Phi(S, t) = \begin{bmatrix} I \\ C' A^{-1} \end{bmatrix} \Phi(S, t).$$

Let $Z = (D - C'A^{-1}C)^{-1}$. Using the formula for the inverse of a block matrix, we get

$$\begin{aligned}\tilde{H}(t) &= \Phi(S, t)' \begin{bmatrix} I & A^{-1}C \end{bmatrix} \begin{bmatrix} A^{-1} + A^{-1}CZC'A^{-1} & -A^{-1}CZ \\ -ZC'A^{-1} & Z \end{bmatrix} \begin{bmatrix} I \\ C'A^{-1} \end{bmatrix} \Phi(S, t) \\ &= \Phi(S, t)' A^{-1} \Phi(S, t) = \left(\int_t^S \Phi(t, \tau) \tilde{a}(\tau) \Phi(t, \tau)' d\tau \right)^{-1}\end{aligned}$$

This is exactly as in lemma 6 of [Schauer et al. \(2017\)](#).

2.3. Differential equations in constant dimension for evaluating \tilde{r} and \tilde{H}

As seen in the previous subsection, the backward differential equations in lemma 2.4 are on $[0, S]$ in a higher dimension than on $(S, T]$. In case we extend to multiple future observations, the dimension will increase further; the dimension on the segment closest to zero being largest. It turns out that another set of backward differential equations can be derived, which is of constant dimension d (the dimension of the state space of the diffusion) over the whole interval $[0, T]$. This property is maintained when multiple future conditionings are taken into account: the recursion is always in dimension d on $[0, t_n]$. This yields large computational savings. Key to this other recursion is the following assumption, which we assume to hold throughout in this subsection. For a matrix A denote its null-space by $\mathcal{N}(A)$.

Assumption 2.8. For all $t \in [0, T]$, $\mathcal{N}(\tilde{L}(t)) = \{0\}$.

From (2.4) it follows that this is essentially an assumption for $t \in (S, T]$ only, as for $t \in [0, S]$ it can be ensured to hold by choice of $\tilde{B}(t)$. The assumption implies that $\mathcal{N}(\tilde{H}(t)) = \{0\}$ and henceforth that the process defined by $\tilde{H}^\dagger(t) = \tilde{H}(t)^{-1}$ exists on $(S, T]$. This in turn implies that \tilde{r} can be written as

$$\tilde{r}(t, x) = \tilde{H}(t)(\nu(t) - x),$$

where

$$\nu(t) = \tilde{H}^\dagger(t) \tilde{L}(t)' \tilde{M}(t) (x_{\text{obs}}(t) - \mu(t)).$$

The following two lemmas show recursions for both $\tilde{H}^\dagger(t)$ and $\nu(t)$.

Lemma 2.9. For $t \in (S, T]$,

$$\frac{d\tilde{H}^\dagger(t)}{dt} = \tilde{B}(t)\tilde{H}^\dagger(t) + \tilde{H}^\dagger(t)\tilde{B}(t)' - \tilde{a}(t), \quad \tilde{H}^\dagger(T) = (L_T'\Sigma_T^{-1}L_T)^{-1}. \quad (2.11)$$

On $[0, S]$ the same differential equation holds, where $\tilde{H}^\dagger(S)$ can be obtained from $\tilde{H}^\dagger(S+)$ from the relation

$$\tilde{H}^\dagger(S) = \tilde{H}^\dagger(S+) - \tilde{H}^\dagger(S+)L_S' \left(\Sigma_S + L_S\tilde{H}^\dagger(S+)L_S' \right)^{-1} L_S\tilde{H}^\dagger(S+) \quad (2.12)$$

Proof. The derivation of the differential equation is the same whether we consider $t \in [0, S]$ or $t \in (S, T]$. Differentiating (2.5) gives

$$\begin{aligned}\frac{d\tilde{H}(t)}{dt} &= \left(\frac{d}{dt} \tilde{L}(t) \right)' \tilde{M}(t) \tilde{L}(t) + \tilde{L}(t)' \left(\frac{d}{dt} \tilde{M}(t) \right) \tilde{L}(t) + \tilde{L}(t)' \tilde{M}(t) \frac{d}{dt} \tilde{L}(t) \\ &= -\tilde{B}(t)' \tilde{L}(t)' \tilde{M}(t) \tilde{L}(t) + \tilde{L}(t)' \left(\frac{d}{dt} \tilde{M}(t) \right) \tilde{L}(t) - \tilde{L}(t)' \tilde{M}(t) \tilde{L}(t) \tilde{B}(t) \\ &= -\tilde{B}(t)' \tilde{H}(t) - \tilde{H}(t) \tilde{B}(t) + \tilde{L}(t)' \left(\frac{d}{dt} \tilde{M}(t) \right) \tilde{L}(t).\end{aligned}$$

Here we use (2.7) at the first equality. We have

$$\frac{d\tilde{M}(t)}{dt} = -\tilde{M}(t) \left(\frac{d}{dt} \tilde{M}^\dagger(t) \right) \tilde{M}(t) = \tilde{M}(t) \tilde{L}(t) \tilde{a}(t) \tilde{L}(t)' \tilde{M}(t). \quad (2.13)$$

This gives

$$\tilde{L}(t)' \frac{d\tilde{M}(t)}{dt} \tilde{L}(t) = \tilde{H}(t) \tilde{a}(t) \tilde{H}(t).$$

Hence we get

$$\begin{aligned} \frac{d\tilde{H}^\dagger(t)}{dt} &= -\tilde{H}^\dagger(t) \left(\frac{d}{dt} \tilde{H}(t) \right) \tilde{H}^\dagger(t) \\ &= \tilde{H}^\dagger(t) \tilde{B}(t)' + \tilde{B}(t) \tilde{H}^\dagger(t) - \tilde{a}(t). \end{aligned} \quad (2.14)$$

The result now follows from substituting (2.8) and the definition of $\tilde{H}^\dagger(t)$.

To derive (2.12), first note that

$$\begin{aligned} \tilde{H}(S) &= \begin{bmatrix} L_S \\ L_T \Phi(T, S) \end{bmatrix}' \tilde{M}(S) \begin{bmatrix} L_S \\ L_T \Phi(T, S) \end{bmatrix} \\ &= \begin{bmatrix} L_S \\ L_T \Phi(T, S) \end{bmatrix}' \begin{bmatrix} \Sigma_S & 0 \\ 0 & \tilde{M}(S+) \end{bmatrix}^{-1} \begin{bmatrix} L_S \\ L_T \Phi(T, S) \end{bmatrix} \\ &= L_S' \Sigma_S^{-1} L_S + \tilde{H}(S+). \end{aligned}$$

The stated expression now follows from Woodbury's formula. \square

Lemma 2.10. For $t \in (S, T]$,

$$\frac{d\nu(t)}{dt} = \tilde{B}(t)\nu(t) + \tilde{\beta}(t), \quad \nu(T) = (L_T' \Sigma_T^{-1} L_T)^{-1} L_T' \Sigma_T^{-1} v_T. \quad (2.15)$$

On $[0, S]$ the same differential equation holds, where $\nu(S)$ can be obtained from $\nu(S+)$ from the relation

$$\nu(S) = \tilde{H}^\dagger(S) \left(L_S' \Sigma_S^{-1} v_S + \tilde{H}(S+)\nu(S+) \right). \quad (2.16)$$

Proof. The derivation of the differential equation is the same whether we consider $t \in [0, S]$ or $t \in (S, T]$. We have, using (2.11), (2.13) and (2.7)

$$\frac{d}{dt} \left(\tilde{H}^\dagger(t) \tilde{L}(t)' \tilde{M}(t) \right) = \tilde{B}(t) \tilde{H}^\dagger(t) \tilde{L}(t)' \tilde{M}(t).$$

Using (2.9) we get

$$\frac{d}{dt} (x_{\text{obs}}(t) - \mu(t)) = \tilde{L}(t) \tilde{\beta}(t).$$

The previous two equations together yield

$$\begin{aligned} \frac{d}{dt} \nu(t) &= \tilde{B}(t) \tilde{H}^\dagger(t) \tilde{L}(t)' \tilde{M}(t) (x_{\text{obs}}(t) - \mu(t)) + \tilde{H}^\dagger(t) \tilde{L}(t)' \tilde{M}(t) \tilde{L}(t) \tilde{\beta}(t) \\ &= \tilde{B}(t) \nu(t) + \tilde{\beta}(t). \end{aligned}$$

The value of $\nu(T)$ follows from $\tilde{H}^\dagger(T) = (L_T' \Sigma_T^{-1} L_T)^{-1}$, $\tilde{L}(T) = L_T$, $\tilde{M}(T) = \Sigma_T^{-1}$, $x_{\text{obs}}(T) = v_T$ and $\mu(T) = 0$.

To obtain the expression for $\nu(S)$, note that

$$\begin{aligned}
\nu(S) &= \tilde{H}^\dagger(S) \tilde{L}'_S \tilde{M}(S) (x_{\text{obs}}(S) - \mu(S)) \\
&= \tilde{H}^\dagger(S) \begin{bmatrix} L_S \\ \tilde{L}(S+) \end{bmatrix} \begin{bmatrix} \Sigma_S & 0 \\ 0 & \tilde{M}(S+) \end{bmatrix}^{-1} \left(\begin{bmatrix} v_S \\ x_{\text{obs}}(S+) \end{bmatrix} - \begin{bmatrix} 0 \\ \int_s^T L_T \Phi(T, \tau) \tilde{\beta}(\tau) d\tau \end{bmatrix} \right) \\
&= \tilde{H}^\dagger(S) \left(L'_S \Sigma_S^{-1} v_S + \tilde{L}(S+) \tilde{M}(S+) (x_{\text{obs}}(S+) - \mu(S+)) \right) \\
&= \tilde{H}^\dagger(S) \left(L'_S \Sigma_S^{-1} v_S + \tilde{H}(S+) \nu(S+) \right).
\end{aligned}$$

□

Remark 2.11. We investigate the behaviour of $\tilde{H}^\dagger(S)$ and $\nu(S)$ when the noise level tends to zero. Assume $L_S \tilde{H}^\dagger(S+) L'_S$ is invertible. Then it follows from (2.12) that the expression for $\tilde{H}^\dagger(S)$ is also well defined when $\|\Sigma\| \rightarrow 0$. Moreover, when $\Sigma = 0$ we have

$$L_S \tilde{H}^\dagger(S) = L_S \tilde{H}^\dagger(S+) - L_S \tilde{H}^\dagger(S+) L'_S \left(L_S \tilde{H}^\dagger(S+) L'_S \right)^{-1} L_S \tilde{H}^\dagger(S+) = 0.$$

To investigate the limiting behaviour of $\nu(S)$, we write

$$L_S \nu(S) = L_S \tilde{H}^\dagger(S) L'_S \Sigma_S^{-1} v_S + L_S \tilde{H}^\dagger(S) \tilde{H}(S+) \nu(S+).$$

The second term on the right-hand-side is easily seen to tend to zero when $\|\Sigma_S\| \rightarrow 0$. For deriving the limit of the first term on the right-hand-side we define $C = L_S \tilde{H}^\dagger(S+) L'_S \Sigma_S^{-1}$ and rewrite

$$\begin{aligned}
L_S \tilde{H}^\dagger(S) L'_S \Sigma_S^{-1} &= L_S \tilde{H}^\dagger(S+) L'_S \Sigma_S^{-1} \\
&\quad - L_S \tilde{H}^\dagger(S+) L'_S \left(\Sigma_S + L_S \tilde{H}^\dagger(S+) L'_S \Sigma_S^{-1} \Sigma_S \right)^{-1} L_S \tilde{H}^\dagger(S+) L'_S \Sigma_S^{-1} \\
&= C - C(I + C)^{-1} C = (I + C^{-1})^{-1},
\end{aligned}$$

where we used Woodbury's formula at the final equality. Now

$$C^{-1} = \Sigma_S \left(L_S \tilde{H}^\dagger(S+) L'_S \right)^{-1} \rightarrow 0, \quad \text{when } \|\Sigma_S\| \rightarrow 0.$$

This implies that $L_S \tilde{H}^\dagger(S) L'_S \Sigma_S^{-1} \rightarrow I$. Combining these results we obtain that

$$L_S \nu(S) \rightarrow v_S, \quad \text{when } \|\Sigma_S\| \rightarrow 0.$$

In particular, if we have full observations at time S , i.e. $L_S = I$, then $\tilde{H}^\dagger(S) \rightarrow 0$ and $\nu(S) \rightarrow v_S$ if $\|\Sigma_S\| \rightarrow 0$. As a consequence, in case of full observations and no noise, we recover the full observation without noise case (in this simpler setting, the differential equations for ν and \tilde{H}^\dagger were derived in [van der Meulen and Schauer \(2017c\)](#)). However, in the general case where L_S is not of full rank, we need that $\det \Sigma_S \neq 0$ to obtain the value of $\nu(S)$ from $\nu(S+)$.

3. Multiple future conditionings

The results of subsection 2.2 can be generalised to the case where we condition on future incomplete observations $V_i = v_i$ at times t_i ($1 \leq i \leq n$). Suppose $t \in (t_{i-1}, t_i]$, then we have

$$\Upsilon(t) = \text{diag}(\Sigma_i, \dots, \Sigma_n)$$

$$\tilde{L}(t) = \begin{bmatrix} L_i \Phi(t_i, t) \mathbf{1}_{[0, t_i]}(t) \\ L_{i+1} \Phi(t_{i+1}, t) \mathbf{1}_{[0, t_{i+1}]}(t) \\ \vdots \\ L_n \Phi(t_n, t) \mathbf{1}_{[0, t_n]}(t) \end{bmatrix}$$

$$\mu(t) = \int_t^{t_n} \tilde{L}(\tau) \tilde{\beta}(\tau) d\tau.$$

The differential equations of lemma 2.4 are still valid. The relations in (2.10) can be generalised to

$$\tilde{L}(t_i) = \begin{bmatrix} 0_{m_i \times d} \\ \tilde{L}(t_{i+}) \end{bmatrix} \quad \tilde{M}^\dagger(t_i) = \text{diag}(\Sigma_1, \dots, \Sigma_i, \tilde{M}^\dagger(t_{i+})) \quad \mu(t_i) = \begin{bmatrix} 0_{m_i \times d} \\ \mu(t_{i+}) \end{bmatrix}. \quad (3.1)$$

The results from subsection 2.3 can also be generalised. It is easily seen that equations (2.11) and (2.15) hold in general. The transitions at observation times t_i are exactly as in lemmas 2.9 and 2.10. They are given in section 5.

4. Understanding the backward scheme

Here, we provide some intuition on the backward scheme for $\tilde{H}^\dagger(t)$ and $\nu(t)$. Denote \tilde{X}_{t_i} by \tilde{X}_i . Using “Bayesian notation”, we have

$$\begin{aligned} p(\tilde{X}_i | V_i, \dots, V_n) &\propto p(V_i | \tilde{X}_i, V_{i+1}, \dots, V_n) p(\tilde{X}_i | V_{i+1}, \dots, V_n) \\ &= p(V_i | \tilde{X}_i) p(\tilde{X}_i | V_{i+1}, \dots, V_n) \end{aligned}$$

which is valid for all $i = 0, \dots, n-1$. Now clearly

$$\begin{aligned} V_i | \tilde{X}_i &\sim N(L_i \tilde{X}_i, \Sigma_i) \\ \tilde{X}_i | V_{i+1}, \dots, V_n &\sim N(\nu(t_i+), \tilde{H}^\dagger(t_i+)) \end{aligned}$$

From these laws, we find that $\tilde{X}_i | V_i, \dots, V_n$ is normally distributed with mean $\nu(t_i)$ and covariance matrix $\tilde{H}^\dagger(t_i)$ and their values can indeed be obtained from equations (2.12) and (2.16).

For $i = n$, which yields $\nu(t_n)$ and $\tilde{H}^\dagger(t_n)$, note that

$$p(\tilde{X}_n | V_n) \propto p(V_n | \tilde{X}_n) p(\tilde{X}_n).$$

From this expression we find that if we assume $p(\tilde{X}_n) \propto 1$ (the improper uniform prior), then

$$\tilde{X}_n | V_n = v_n \sim N\left(\nu(t_n), \tilde{H}^\dagger(t_n)\right) \quad (4.1)$$

with

$$\tilde{H}^\dagger(t_n) = (L'_n \Sigma_n^{-1} L_n)^{-1} \quad \text{and} \quad \nu(t_n) = \tilde{H}^\dagger(t_n) L'_n \Sigma_n^{-1} v_n.$$

This corresponds exactly to the initialisation $\tilde{H}^\dagger(t_n+) = 0$ and $\nu(t_n+) = 0$ (using equations (2.12) and (2.16)).

In case we assume \tilde{X}_n to have the $N(\kappa, C)$ -distribution, we obtain (4.1) with

$$\begin{aligned} \tilde{H}^\dagger(t_n) &= (L'_n \Sigma_n^{-1} L_n + C^{-1})^{-1} \\ \nu(t_n) &= \tilde{H}^\dagger(t_n) (L'_n \Sigma_n^{-1} v_n + C^{-1} \kappa). \end{aligned} \quad (4.2)$$

Again, these values can be obtained from the update equations (2.12) and (2.16); this time by defining

$$\nu(t_n+) = \kappa \quad \text{and} \quad \tilde{H}^\dagger(t_n+) = C. \quad (4.3)$$

This choice is particularly relevant in case $L'_n \Sigma_n^{-1} L_n$ is not invertible, as taking $C^{-1} \neq 0$ ensures existence of $\tilde{H}^\dagger(t)$ and henceforth has a regularising effect.

One way to view (4.3), is by imagining the inclusion of an artificial observation immediately after the time of the last observation. Denote this time by t_n+ . Now suppose at time t_n+ we have the observation V_{n+} satisfying $V_{n+} = \kappa + \eta_{n+}$, where $\eta_{n+} \sim N(0, C)$. This corresponds to fully observing the process at time t_n+ with value κ with $N(0, C)$ -noise superimposed. This extra artificial observation V_{n+} regularises the case of partial observations as it always ensures that the final (real albeit artificial) observation is fully observed with noise. In this way it is ensured that assumption 2.8 is satisfied on the “interval” including the last observation.

We will choose $\kappa = 0$ and $C^{-1} = \varepsilon I_d$, where $\varepsilon \in [0, \infty)$. In case the final observation is fully observed, one can take $\varepsilon = 0$, else a small value can be taken.

5. A novel smoothing algorithm

In this section we use the differential equations for \tilde{H}^\dagger and ν derived in section 2.3 to derive an algorithm for continuous-discrete smoothing of diffusions. The algorithm assumes the addition of an artificial observation $V_{n+} \sim N(0, \varepsilon^{-1} I)$ as explained in section 4. Furthermore, a preconditioned Crank-Nicolson scheme is used (Cf. Cotter et al. (2013) and Beskos et al. (2008)). Recall that assumption 2.1 ensures the existence of a measurable map g such that $X^\circ = g(X_0, W)$, where W is a Wiener process in $\mathbb{R}^{d'}$.

We propose the following algorithm:

Algorithm 5.1. Choose a regularisation parameter $\varepsilon \geq 0$ and a persistence parameter $\lambda \in [0, 1)$. Denote the number of MCMC iterations by N .

1. Initialise

$$\begin{aligned} \tilde{H}^\dagger(t_n) &= (L'_n \Sigma_n^{-1} L_n + \varepsilon I)^{-1} \\ \nu(t_n) &= \tilde{H}^\dagger(t_n) L'_n \Sigma_n^{-1} v_n. \end{aligned}$$

2. For $i = n - 1$ to 0

- (a) For $t \in (t_i, t_{i+1}]$, backwards solve the ordinary differential equations

$$\begin{aligned} \frac{d\tilde{H}^\dagger(t)}{dt} &= \tilde{B}(t)\tilde{H}^\dagger(t) + \tilde{H}^\dagger(t)\tilde{B}(t)' - \tilde{a}(t), \\ \frac{d\nu(t)}{dt} &= \tilde{B}(t)\nu(t) + \tilde{\beta}(t). \end{aligned}$$

- (b) Compute

$$\begin{aligned} \tilde{H}^\dagger(t_i) &= \tilde{H}^\dagger(t_{i+1}) - \tilde{H}^\dagger(t_{i+1}) L'_i \left(\Sigma_i + L_i \tilde{H}^\dagger(t_{i+1}) L'_i \right)^{-1} L_i \tilde{H}^\dagger(t_{i+1}), \\ \nu(t_i) &= \tilde{H}^\dagger(t_i) \left(L'_i \Sigma_i^{-1} v_i + \tilde{H}(t_{i+1}) \nu(t_{i+1}) \right). \end{aligned}$$

3. Sample $X_0 \sim N(\nu(0), \tilde{H}^\dagger(0))$ and a Wiener process Z on $[0, t_n]$. Simulate the guided proposal $X^\circ = g(X_0, Z)$, i.e.

$$dX_t^\circ = \left(b(t, X_t^\circ) + a(t, X_t^\circ) \tilde{H}(t)(\nu(t) - X_t^\circ) \right) dt + \sigma(t, X_t^\circ) dZ_t.$$

Initialise X by defining $X = (X_t^\circ, t \in [0, t_n])$.

4. Repeat N times

- (a) Propose a new value for X_0° as follows

$$X_0^\circ = \nu(0) + \sqrt{\lambda}(X_0 - \nu(0)) + \sqrt{1 - \lambda}Z,$$

with $Z \sim N(0, \tilde{H}^\dagger(0))$. Sample independently a Wiener process W and set

$$Z^\circ = \sqrt{\lambda}Z + \sqrt{1 - \lambda}W.$$

Compute

$$X^\circ = g(X_0^\circ, Z^\circ).$$

- (b) Compute

$$A = \Psi(X^\circ)\Psi(X)^{-1},$$

where Ψ is as defined in (2.2). Draw $U \sim \mathcal{U}(0, 1)$. If $U < A$ then set $X = X^\circ$ and $Z = Z^\circ$.

In steps (1) and (2) $\tilde{H}^\dagger(t)$ and $\nu(t)$ are calculated for $t \in [t_0, t_n]$; the formulas follow directly from lemmas 2.9 and 2.10. Once these have been calculated and stored (on a fine grid), the remainder of the algorithm consists of steps where first the driving Wiener increments of X° are perturbed, then the process X° is simulated forward and finally the acceptance probability is evaluated. After “burnin”, the sample paths generated by this algorithm are from the smoothing distribution.

Lemma 5.2. Algorithm 5.1 targets the distribution of $(X_t, t \in [0, t_n])$, conditional on the observations D .

Proof. We use “Bayesian notation”. Write $X_{(0:n]} = (X_t, t \in (0, t_n])$ and $X_{[0:n]} = (X_t, t \in [0, t_n])$. The target density can be factorised as

$$p(X_{[0:n]} | D) = p(X_{(0:n]} | X_0, D)p(X_0 | D).$$

The proposal $X_{[0:n]}^\circ$ is defined by

$$q(X_{[0:n]}^\circ | X_{[0:n]}, D) = q(X_0^\circ | X_0, D)q(X_{(0:n]}^\circ | X_0^\circ, X_{(0:n]}, D).$$

Let \tilde{p} refer to conditional densities for the auxiliary process \tilde{X} . By choice of the update for \tilde{X} we have

$$\frac{q(X_0^\circ | X_0, D) \tilde{p}(X_0 | D)}{q(X_0 | X_0^\circ, D) \tilde{p}(X_0^\circ | D)} = 1. \quad (5.1)$$

This can be seen as follows: if we sample (X_0, X_0°) according to the densities in the numerator, then

$$\begin{aligned} X_0 &\sim N(\nu(0), \tilde{H}^\dagger(0)) \\ X_0^\circ | X_0 &\sim N\left(\nu(0) + \sqrt{\lambda}(X_0 - \nu(0)), (1 - \lambda)\tilde{H}^\dagger(0)\right) \end{aligned}$$

By elementary properties of the normal distribution it follows that

$$\begin{bmatrix} X_0 \\ X_0^\circ \end{bmatrix} \sim N \left(\begin{bmatrix} \nu(0) \\ \nu(0) \end{bmatrix}, \begin{bmatrix} \tilde{H}^\dagger(0) & \sqrt{\lambda} \tilde{H}^\dagger(0) \\ \sqrt{\lambda} \tilde{H}^\dagger(0) & \tilde{H}^\dagger(0) \end{bmatrix} \right)$$

(see for instance lemma A.1 on page 209 in [Särkkä \(2013\)](#)). Therefore, the proposal on X_0 satisfies detailed balance for the target distribution $\tilde{p}(X_0 | D)$ for any $\lambda \in [0, 1)$. Similarly, the acceptance probability for the update Z_{new} is the same for any $\lambda \in [0, 1)$. Without loss of generality we therefore assume $\lambda = 0$.

The acceptance probability for the update from $X_{[0:n]}$ to $X_{[0:n]}^\circ$ equals $1 \wedge A$, where

$$A = \frac{p(X_{[0:n]}^\circ | X_0^\circ, D) p(X_0^\circ | D) q(X_0 | X_0^\circ, D) q(X_{[0:n]} | X_0, X_{[0:n]}^\circ, D)}{p(X_{[0:n]} | X_0, D) p(X_0 | D) q(X_0^\circ | X_0, D) q(X_{[0:n]}^\circ | X_0^\circ, X_{[0:n]}, D)}$$

Now

$$\frac{p(X_{[0:n]}^\circ | X_0^\circ, D)}{q(X_{[0:n]}^\circ | X_0^\circ, X_{[0:n]}, D)} = \frac{\tilde{\rho}(0, X_0^\circ)}{\rho(0, X_0^\circ)} \Psi(X_{[0:n]}^\circ)$$

Note that $\rho(0, X_0) = p(X_0 | D)$ and $\tilde{\rho}(0, X_0) = \tilde{p}(X_0 | D)$. Using these equalities, preceding display and (5.1), the expression for A can be simplified to

$$\begin{aligned} A &= \frac{\tilde{\rho}(0, X_0^\circ)}{\rho(0, X_0^\circ)} \Psi(X_{[0:n]}^\circ) \left(\frac{\tilde{\rho}(0, X_0)}{\rho(0, X_0)} \Psi(X_{[0:n]}) \right)^{-1} \frac{\rho(0, X_0^\circ)}{\rho(0, X_0)} \frac{\tilde{p}(X_0 | D)}{\tilde{p}(X_0^\circ | D)} \\ &= \Psi(X_{[0:n]}^\circ) / \Psi(X_{[0:n]}). \end{aligned}$$

This is exactly as specified in step 4(b) of the algorithm. \square

While the algorithm is theoretically valid for any fixed value of λ , its efficiency strongly depends on the particular choice of this parameter. Instead of a fixed value of λ , we can choose it randomly in each iteration of step (4): the acceptance probability in step (5) is not affected by its value (Cf. the discussion after algorithm 1 in [van der Meulen and Schauer \(2017a\)](#)).

Remark 5.3. In case there are unknown parameters in either the drift or dispersion coefficient, or the covariance matrices Σ_i ($0 \leq i \leq n$) cannot be assumed known, then a data-augmentation algorithm can be used. This entails iteratively sampling from the unknown parameters conditional on the smoothed path, followed by the presented smoothing algorithm with the current values of the parameters. This approach is well known in the present setting and goes back to the seminal paper by [Roberts and Stramer \(2001\)](#). For a general discussion on this we refer to [van der Meulen and Schauer \(2017a\)](#).

Remark 5.4. If the measurement error is close to zero, then the (Euler) discretisation of the guided proposal is a delicate matter due to the behaviour of the guiding term just prior to observation times. As discussed in section 5 of [van der Meulen and Schauer \(2017a\)](#) a time change and scaling of the process can alleviate discretisation errors. For completeness, we present this approach in appendix A.

Remark 5.5. Suppose in between two adjacent time points t_i and t_{i+1} we use m imputed points. Saving the values of $\nu(t)$ and $\tilde{H}^\dagger(t)$ on the grid then requires saving approximately $mnd^2/2$ real numbers. To see this: by symmetry of $\tilde{H}^\dagger(t)$, saving both $\tilde{H}^\dagger(t)$ and $\nu(t)$ at one particular point requires saving $d(d-1)/2 + d$ real numbers. This is to be multiplied with the number of points on the grid, which is $\mathcal{O}(mn)$.

5.1. Choice of the auxiliary process \tilde{X}

The algorithm requires choosing the auxiliary process \tilde{X} , i.e. the parameters $\tilde{\beta}(t)$, $\tilde{B}(t)$ and $\tilde{\sigma}(t)$. A number of practical ways for doing this are discussed in [van der Meulen and Schauer \(2017a\)](#) (section 4.4). We present a number of ways for doing this:

- A Waive the freedom and simply take $\tilde{\sigma}$ constant, $\tilde{B}(t) \equiv 0$ and $\tilde{\beta} = 0$. Under regularity conditions on σ , L and Σ this yields a valid algorithm, which still takes the local nonlinearity into account through the presence of b in (1.4).
- B Choose $\tilde{\sigma} = \sigma$, $\tilde{B}(t) \equiv 0$ and take $\tilde{\beta}$ nonzero to take the nonlinearity in the system also into account in the pulling term. To determine $\tilde{\beta}$, we propose to first solve $\nu(t_n)$ from

$$L'_n \Sigma_n^{-1} L_n \nu(t_n) = L'_n \Sigma_n^{-1} v_n.$$

Next, for $i = n$ to 1:

- (a) For $t \in (t_{i-1}, t_i]$, backwards solve

$$dx(t) = b(t, x(t)) dt, \quad x(t_i) = \nu(t_i).$$

Set $\tilde{\beta}(t) = b(t, x(t))$.

- (b) Compute $\nu(t)$ for all $t \in (t_{i-1}, t_i]$. Compute $\nu(t_{i-1})$ using $\nu(t_{i-1}+)$ using (2.16).

- C Adaptively improve upon the auxiliary process. We give a more elaborate way to choose \tilde{B} and $\tilde{\beta}$ adaptively which does not require to treat different drift functions in a case specific way. The overall idea is to determine $\bar{x}(t) = \mathbb{E}[X_t | D]$ and do a first order Taylor expansion $\tilde{b}(t, x) = b(t, \bar{x}(t)) + J_b(t, \bar{x}(t))(x - \bar{x}(t))$ where J_b denotes the Jacobian matrix of b . Of course $\bar{x}(t)$ is unknown, but information becomes available during MCMC-iterations.

More specifically, we propose to first use the auxiliary process constructed by one of the preceding methods to get $\tilde{b}^{(0)}(t, x) = \tilde{\beta}(t) + \tilde{B}(t)x$. Next, run the algorithm for k iterations and compute the average of these k paths. Denote this average by $\{\bar{X}^{(0)}(t), t \in [0, t_n]\}$. Next, starting at $i = 1$, repeat the following steps until the prescribed total number of iterations has been reached.

- (a) Set

$$\tilde{b}^{(i)}(t, x) = b(t, \bar{X}^{(i-1)}(t)) + J_b(t, \bar{X}^{(i-1)}(t)) (x - \bar{X}^{(i-1)}(t)).$$

- (b) Recompute $\tilde{H}^\dagger(t)$ and $\nu(t)$ on $[0, t_n]$ based on $\tilde{b}^{(i)}(t, x)$.
- (c) Perform k MCMC-iterations based on $\tilde{H}^\dagger(t)$ and $\nu(t)$. Compute the average of all simulated paths to obtain $\{\bar{X}^{(i)}(t), t \in [0, t_n]\}$

This adaptive scheme has diminishing adaptation. While a formal proof is not within the scope of this article, simulation results indicate that this method offers an effective automatic way for choosing the auxiliary process.

Methods A and B always give a valid algorithm for uniformly elliptic diffusions, though may be very inefficient.

6. Examples

In all examples, the differential equations for $\nu(t)$ and $\tilde{H}^\dagger(t)$ have been solved using a Runge-Kutta scheme with the Ralston tableau ([Ralston \(1965\)](#)). The guided proposal is obtained by

solving its SDE using Euler-discretisation. The code is available in the folder **supplements** of the package *Bridge* (Schauer and contributors (2017)) for the programming language Julia (Bezanson et al. (2017)).

6.1. Lorenz system

The Lorenz system is notable for having chaotic solutions for certain parameter values and initial conditions. It is described by the SDE with drift and dispersion coefficient given by

$$b(x) = \begin{bmatrix} \theta_1(x_2 - x_1) \\ \theta_2 x_1 - x_2 - x_1 x_3 \\ x_1 x_2 - \theta_3 x_3 \end{bmatrix} \quad \text{and} \quad \sigma = \sigma_0 I_{3 \times 3}.$$

Data: We simulated the process on $[0, 4]$ with mesh-width $8\text{e-}5$ and retained 101 observations at times $0, 0.04, 0.08, \dots, 4$. We took $\theta = [10 \ 28 \ 8/3]'$, $\sigma_0 = 3$ and $\Sigma_i = I$ as covariance matrix for the noise. The process was initialised at $x_0 = [1.508870 \ -1.531271 \ 25.46091]'$. The simulated path and observed data are shown in figure 1.

Algorithm details: We sample λ randomly at each iteration. As we wish to assign more probability to values of λ close to 1 compared to 0, we chose $\lambda \sim \text{Beta}(1, \alpha)$ which is a simple and pragmatic approach. We took as regularisation parameter $\varepsilon^{-1} = 2000$. Every 10^3 iterations we adjust the auxiliary process based on the mean of the past samples. Only the first time an adaptive update is performed the algorithm is set to automatically accept the proposal.

We ran the MCMC-sampler for 10^6 -iterations using methods A, B and C for choosing the auxiliary process \tilde{X} . For methods A and B we took $\alpha = 5$, resulting in average acceptance probabilities of 0.24 and 0.26 respectively. This corresponds to small incremental updates. For method C we took $\alpha = 0.5$ resulting in the average acceptance probability 0.89. This is close to an independence sampler. Each simulation run took about 20 minutes on a machine with an Intel Core M 1.1 GHz processor with 2 cores.

In figures 2, 3 and 4 we show traceplots and autocorrelation plots for the smoothed value at $t = 2$. The brown dashed lines in the traceplots indicate the values of the simulated path of the diffusion. As we only have one realisation of the path and finitely many observations, the conditional distribution (given the data) is not centred at this line. However, we can expect the samples to be close to these lines. More definitive information about the location of the conditional distribution is provided by the location of the samples in figure 4, where the chain certainly has reached its equilibrium. From the trace- and autocorrelation plots it is clear that method C outperforms the other methods substantially. In fact, almost independent samples from the posterior are obtained. For completeness, we also include similar plots at the starting point for method C in figure 5.

In figures 6, 7 and 8 twenty samples of the smoothed path are shown for methods A, B and C respectively. These have been obtained by subsampling the Metropolis-Hastings chains every 5000 steps. In darker colours the sample path used to generate the observations, and the observations themselves, have been added. In figure 6 it can be seen that the blue coloured parts of the samples are not as close to the truth as in the other figures. This is not surprising as the traceplots indicate that the chain has not reached equilibrium yet.

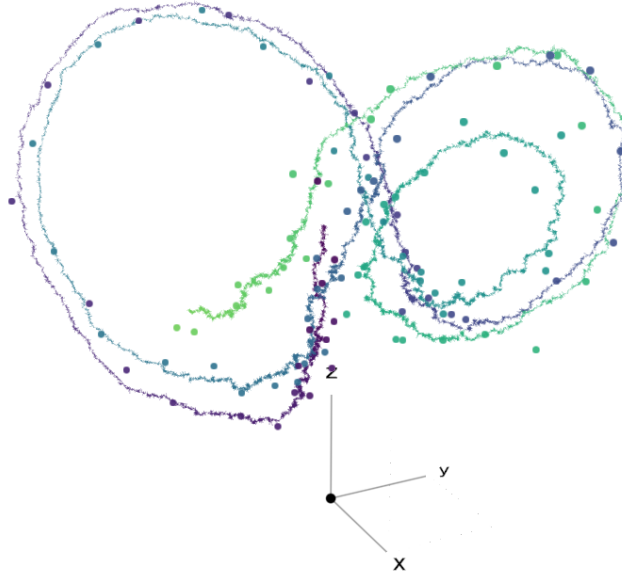


FIGURE 1. *Lorenz system: A sample path of the stochastic Lorenz system on for $t = [0, 4]$, together with 101 equidistant complete observations with standard normal error on the coordinates. Colors indicate progress of time, with $t = 0$ being violet/dark.*

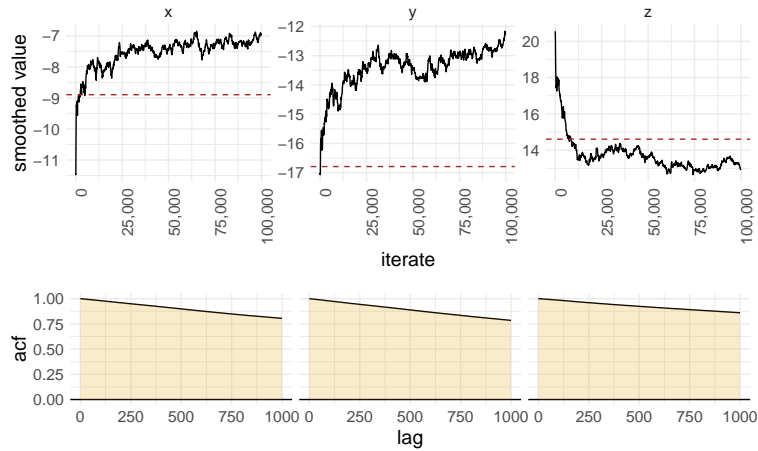


FIGURE 2. *Lorenz system: Traceplots (top) and autocorrelations plots (bottom) of the MCMC iterates for X_2 . Auxiliary process chosen by method [A]. The autocorrelation plots disregard the first 10^4 samples which are treated as burnin samples. The dashed horizontal lines in the traceplots indicate the value of the simulated path.*

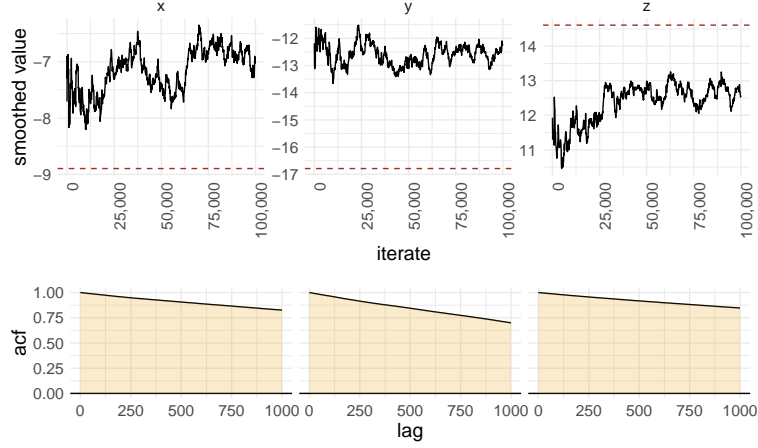


FIGURE 3. Lorenz system: Traceplots (top) and autocorrelations plots (bottom) of the MCMC iterates for X_2 . Auxiliary process chosen by method [B]. The autocorrelation plots disregard the first 10^4 samples which are treated as burnin samples. The dashed horizontal lines in the traceplots indicate the value of the simulated path.

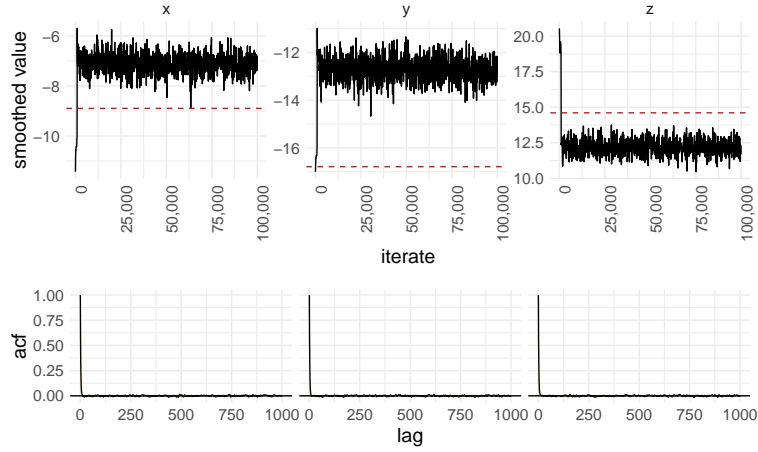


FIGURE 4. Lorenz system: Traceplots (top) and autocorrelations plots (bottom) of the MCMC iterates for X_2 . Auxiliary process chosen by method [C]. The autocorrelation plots disregard the first 10^4 samples which are treated as burnin samples. The dashed horizontal lines in the traceplots indicate the value of the simulated path.

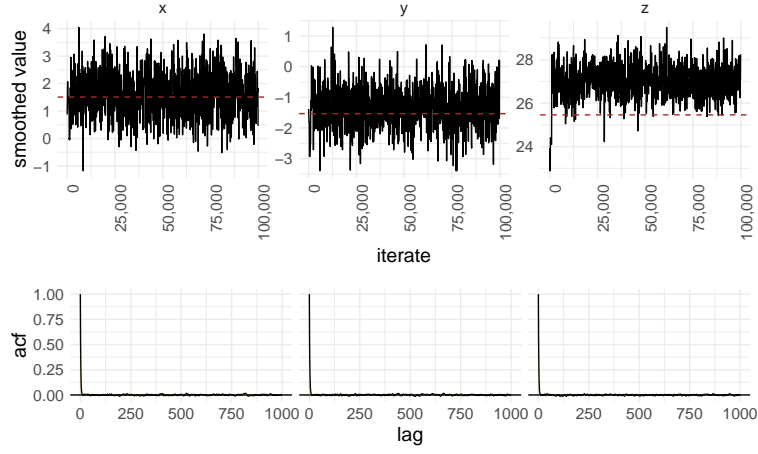


FIGURE 5. *Lorenz system: Traceplots (top) and autocorrelations plots (bottom) of the MCMC iterates for X_0 . Auxiliary process chosen by method [C]. The autocorrelation plots disregard the first 10^4 samples which are treated as burnin samples. The dashed horizontal lines in the traceplots indicate the value of the simulated path.*

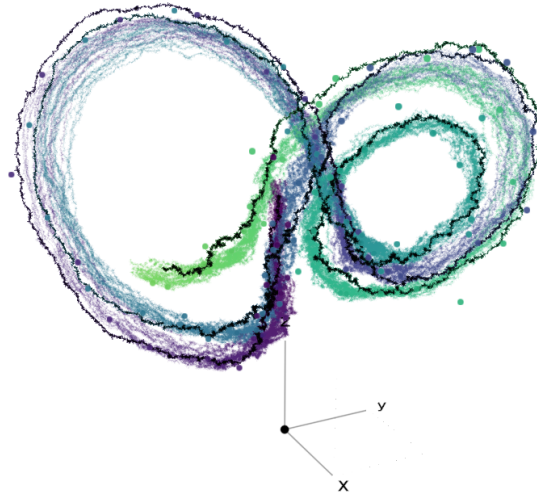


FIGURE 6. *Lorenz system: Twenty samples of the smoothed path, obtained by subsampling the Metropolis-Hastings chain every 5000 steps with method A. In darker colours the sample path used to generate the observations, and the observations themselves, have been added.*

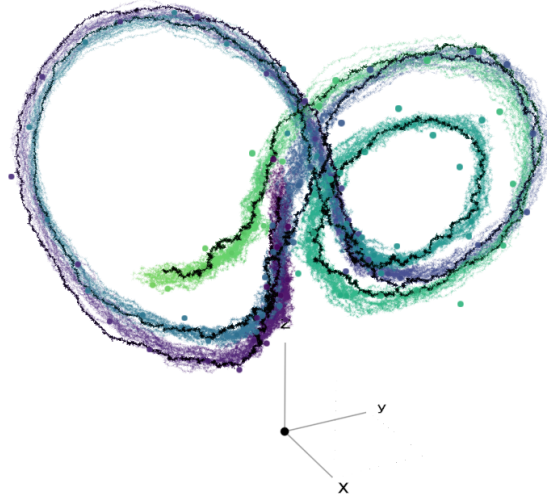


FIGURE 7. *Lorenz system: Twenty samples of the smoothed path, obtained by subsampling the Metropolis-Hastings chain every 5000 steps with method B. In darker colours the sample path used to generate the observations, and the observations themselves, have been added.*

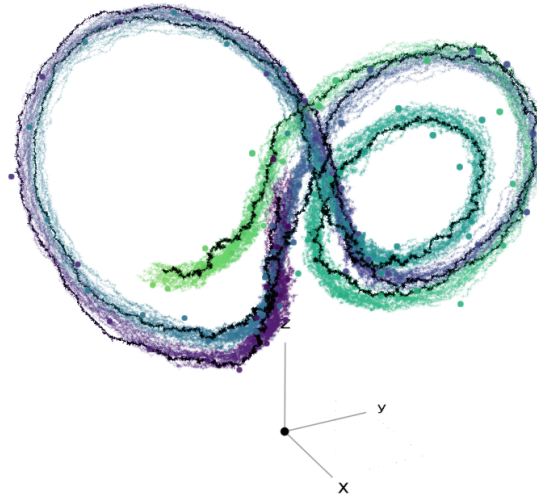


FIGURE 8. *Lorenz system: Twenty samples of the smoothed path, obtained by subsampling the Metropolis-Hastings chain every 5000 steps with method C. In darker colours the sample path used to generate the observations, and the observations themselves, have been added.*

6.2. Simple pendulum

The differential equation for the angular position of a single pendulum is given by

$$\frac{d^2 x(t)}{dt^2} + \theta^2 \sin(x(t)) = 0.$$

Here $x(t)$ gives the angular position at time t and θ is the angular velocity of the linearised pendulum. Under the assumption that the acceleration is in fact a white-noise process, we arrive at the SDE

$$dX_t = \begin{bmatrix} 0 & 1 \\ 0 & 0 \end{bmatrix} X_t dt + \begin{bmatrix} 0 \\ -\theta^2 \sin(X_{1t}) \end{bmatrix} dt + \begin{bmatrix} 0 \\ \gamma \end{bmatrix} dW_t,$$

where $X_t = [X_{t1} \ X_{t2}]'$. This is an example of a two dimensional hypo-elliptic diffusion. It was previously discussed in section 3.1 of [Särkkä and Sottinen \(2008\)](#). Assume the position is observed with noise at times $t_0 < t_1 < \dots < t_n$. This amounts to $L_i = [1 \ 0]$ for all $i = 0, \dots, n$ in our setup.

Data: We simulated the process on $[0, 4]$ with mesh-width $8e-05$ and retained 101 observations at times $0, 0.04, 0.08, \dots, 4$. We took $\theta = 1$, $\gamma = 1$ and considered both $\sigma^2 = 1$ and $\sigma^2 = 0.001$ as variance for the noise on the observations. The process was started at $x_0 = [1 \ 0.5]'$.

Algorithm details: We took as regularisation parameter $\varepsilon^{-1} = 2000$. Every 10^3 iterations we adjust the auxiliary process based on the mean of the past samples. Only the first time an adaptive update is performed the proposal is forced to be automatically accepted.

We ran the MCMC-sampler for 10^6 -iterations, where the auxiliary process was initialised with

$$\tilde{B}(t) = \begin{bmatrix} 0 & 1 \\ 0 & 0 \end{bmatrix} \quad \tilde{\beta}(t) = \begin{bmatrix} 0 \\ 0 \end{bmatrix} \quad \tilde{\sigma} = \begin{bmatrix} 0 \\ \gamma \end{bmatrix}.$$

This choice respects the hypo-elliptic structure of the diffusion in the construction of the guiding term in X° , but fully ignores the nonlinearity. We first discuss the results for $\sigma^2 = 1$. We took $\alpha = 0.5$ resulting in an average acceptance probability of 0.96, respective 0.98. This is close to an independence sampler.

In figure 9 trace- and autocorrelation plots for the smoothed value at time 0 are displayed. For the autocorrelation plots, the first 2000 observations have been discarded. We also made autocorrelation plots at time $t = 2$ and these look similar to those for time $t = 0$. In figure 10 the simulated full path is displayed in yellow and the observations are depicted by red dots. The solid black line is the posterior mean. The grey area is enclosed by the curves located at the posterior mean ± 1.96 times the poster standard deviation (computed at each time instance).

In case $\sigma^2 = 0.001$ the posterior mean is shown in figure 11. Here, the first component is not included as it can almost be recovered exactly due to the relatively high temporal frequency of the observations and low noise on the observations.

Appendix A: Implementation using a time-change and scaling

If the noise level on the observation is small, care is required in the discretisation of guided proposals near the conditioning points. For this reason, a time-change and scaling was introduced in section 5 of [van der Meulen and Schauer \(2017a\)](#). Here, we explain it for the case of

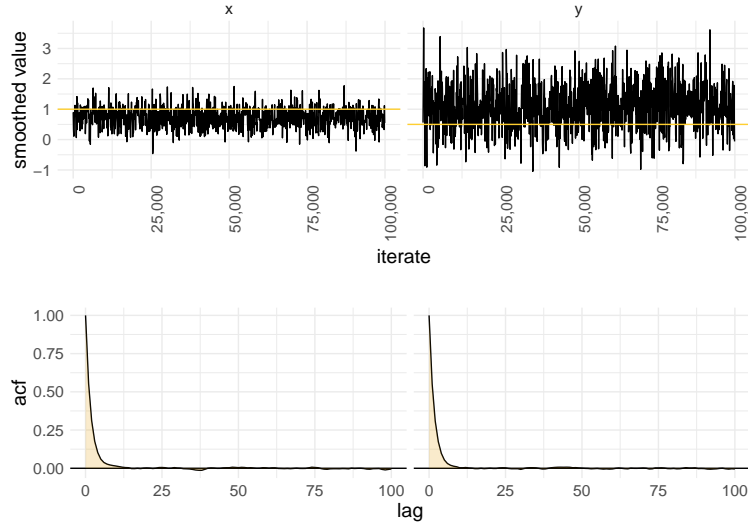


FIGURE 9. Pendulum example: Traceplots (top) and autocorrelations plots (bottom) of the MCMC iterates for X_0 . The data were generated with $\sigma = 1$. Auxiliary process chosen by method C. The autocorrelation plots discard the first 2000 samples which are treated as burnin samples. The horizontal lines in the traceplots indicate the value of the simulated path.

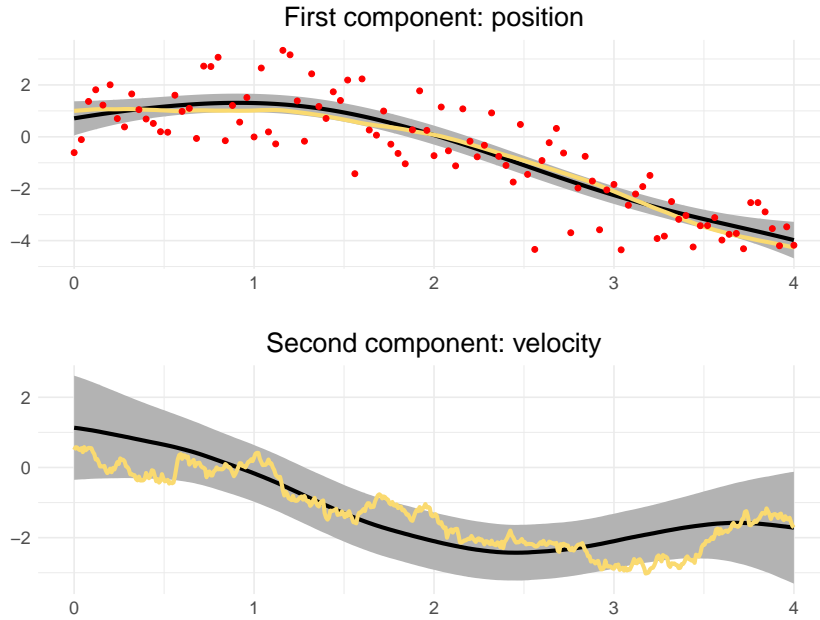


FIGURE 10. Pendulum example: top- and bottom plot display results for the first and second component respectively. The data were generated with $\sigma^2 = 1$. The black line is the posterior mean, the grey areas displays marginal 95%-credible sets using a Normal approximation. The observations are depicted by red points. The yellow curves represent the simulated path.

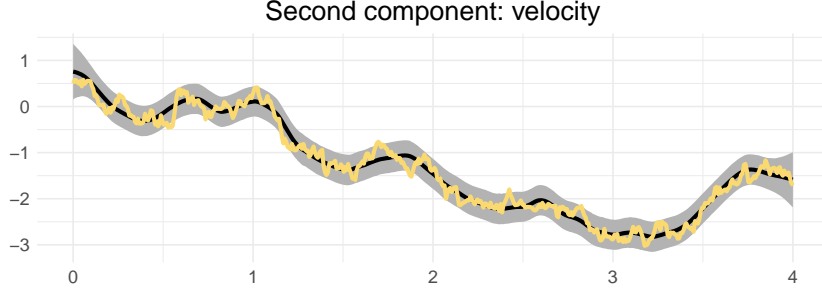


FIGURE 11. *Pendulum example: second component.* The data were generated with $\sigma^2 = 0.001$. The black line is the posterior mean, the grey areas displays marginal 95%-credible sets using a Normal approximation. The observations are depicted by red points. The yellow curves represent the simulated path.

2 future conditionings (as in section 2). Define the mapping $\tau : [0, S + T] \rightarrow [0, S + T]$ by

$$\tau(s) = \begin{cases} s \left(2 - \frac{s}{S}\right) & \text{if } s \in [0, S] \\ S + (s - S) \left(2 - \frac{s-S}{T-S}\right) & \text{if } s \in [S, T] \end{cases}.$$

For a mapping $f : \mathbb{R} \rightarrow \mathbb{R}$ we write $f_\tau(s) = f(\tau(s))$. We propose to discretise the process U_s , defined by

$$U_s = \frac{\nu_\tau(s) - X_{\tau(s)}^\circ}{\dot{\tau}(s)},$$

instead on X_s° . This process satisfies the SDE

$$\begin{aligned} dU_s = & \left(\tilde{B}_\tau(s) v_\tau(s) + \tilde{\beta}_\tau(s) - b_\tau(s, U_s) \right) ds \\ & - \left(\frac{\ddot{\tau}(s)}{\dot{\tau}(s)} I + a_\tau(s, U_s) J(s) \right) U_s ds \\ & + \frac{1}{\sqrt{\dot{\tau}(s)}} \sigma_\tau(s, U_s) dW_s, \quad U_0 = \frac{\nu_\tau(0) - x_0}{2} \end{aligned}$$

Here, J is defined by

$$J(s) = \dot{\tau}(s) \tilde{H}_\tau(s).$$

Furthermore, we have used the notation $b_\tau(s, y) = b(\tau(s), v_\tau(s) - \dot{\tau}(s)y)$ and similarly for σ_τ and a_τ . For the likelihood ratio (2.1), note that $\tilde{r}(\tau(s), X_{\tau(s)}^\circ) = J(s)U_s$.

$$\begin{aligned} \int_0^T G(s, X_s^\circ) ds = & \int_0^T \left(b_\tau(s, U_s) - \tilde{b}_\tau(s, U_s) \right) J(s) U_s \dot{\tau}(s) ds \\ & - \frac{1}{2} \int_0^T \text{tr} \left(\{a_\tau(s, U_s) - \tilde{a}_\tau(s)\} \{J(s) - J(s)U_s U_s' J(s)\} \dot{\tau}(s) \right) ds \end{aligned}$$

Finally, by the chain-rule, $\tilde{H}_\tau^\dagger(s)$ and $\nu_\tau(s)$ satisfy the backward differential equations

$$\frac{d}{dt} \tilde{H}_\tau^\dagger(t) = \left(\tilde{B}_\tau(t) \tilde{H}_\tau^\dagger(t) + \tilde{H}_\tau^\dagger \tilde{B}_\tau(t)' - \tilde{a}_\tau(t) \right) \dot{\tau}(s)$$

and

$$\frac{d}{dt} \nu_\tau(t) = \left(\tilde{B}_\tau(t) \nu_\tau(t) + \tilde{\beta}_\tau(t) \right) \dot{\tau}(s).$$

Acknowledgments

The research leading to the results in this paper has received funding from the European Research Council under ERC Grant Agreement 320637.

References

- Bayer, C. and Schoenmakers, J. (2013). Simulation of forward-reverse stochastic representations for conditional diffusions. *Ann. Appl. Probab.* To appear.
- Beskos, A., Papaspiliopoulos, O., Roberts, G. O. and Fearnhead, P. (2006). Exact and computationally efficient likelihood-based estimation for discretely observed diffusion processes. *J. R. Stat. Soc. Ser. B Stat. Methodol.* **68**(3), 333–382. With discussions and a reply by the authors.
- Beskos, A., Roberts, G., Stuart, A. and Voss, J. (2008). Mcmc methods for diffusion bridges. *Stochastics and Dynamics* **08**(03), 319–350.
- Beskos, A. and Roberts, G. O. (2005). Exact simulation of diffusions. *Ann. Appl. Probab.* **15**(4), 2422–2444.
- Bezanson, J., Edelman, A., Karpinski, S. and Shah, V. B. (2017). Julia: a fresh approach to numerical computing. *SIAM Rev.* **59**(1), 65–98.
- Bladt, M., Finch, S. and Sørensen, M. (2016). Simulation of multivariate diffusion bridges. *J. R. Stat. Soc. Ser. B. Stat. Methodol.* **78**(2), 343–369.
- Clark, J. M. C. (1990). The simulation of pinned diffusions. In *Decision and Control, 1990., Proceedings of the 29th IEEE Conference on*, pp. 1418–1420. IEEE.
- Cotter, S. L., Roberts, G. O., Stuart, A. M. and White, D. (2013). Mcmc methods for functions: Modifying old algorithms to make them faster. *Statist. Sci.* **28**(3), 424–446.
- Delyon, B. and Hu, Y. (2006). Simulation of conditioned diffusion and application to parameter estimation. *Stochastic Processes and their Applications* **116**(11), 1660 – 1675.
- Durham, G. B. and Gallant, A. R. (2002). Numerical techniques for maximum likelihood estimation of continuous-time diffusion processes. *J. Bus. Econom. Statist.* **20**(3), 297–338. With comments and a reply by the authors.
- Elerian, O., Chib, S. and Shephard, N. (2001). Likelihood inference for discretely observed nonlinear diffusions. *Econometrica* **69**(4), 959–993.
- Eraker, B. (2001). MCMC analysis of diffusion models with application to finance. *J. Bus. Econom. Statist.* **19**(2), 177–191.
- Fearnhead, P., Papaspiliopoulos, O. and Roberts, G. O. (2008). Particle filters for partially observed diffusions. *J. R. Stat. Soc. Ser. B Stat. Methodol.* **70**(4), 755–777.
- Fuchs, C. (2013). *Inference for diffusion processes*. Springer, Heidelberg. With applications in life sciences, With a foreword by Ludwig Fahrmeir.
- Golightly, A. and Wilkinson, D. J. (2008). Bayesian inference for nonlinear multivariate diffusion models observed with error. *Comput. Statist. Data Anal.* **52**(3), 1674–1693.
- Hairer, M., Stuart, A. M. and Voss, J. (2009). Sampling conditioned diffusions. In *Trends in Stochastic Analysis*, volume 353 of *London Mathematical Society Lecture Note Series*, pp. 159–186. Cambridge University Press.
- Karatzas, I. and Shreve, S. E. (1991). *Brownian motion and stochastic calculus*, volume 113 of *Graduate Texts in Mathematics*. Springer-Verlag, New York, second edition.
- Lin, M., Chen, R. and Mykland, P. (2010). On generating Monte Carlo samples of continuous diffusion bridges. *J. Amer. Statist. Assoc.* **105**(490), 820–838.
- Lindström, E. (2012). A regularized bridge sampler for sparsely sampled diffusions. *Stat. Comput.* **22**(2), 615–623.

- Marchand, J.-L. (2012). *Conditionnement de processus markoviens*. IRMAR, Ph.d. Thesis Université de Rennes 1.
- Olsson, J. and Ströjby, J. (2011). Particle-based likelihood inference in partially observed diffusion processes using generalised Poisson estimators. *Electron. J. Stat.* **5**, 1090–1122.
- Ralston, A. (1965). *A first course in numerical analysis*. McGraw-Hill Book Co., New York-Toronto-London.
- Roberts, G. O. and Stramer, O. (2001). On inference for partially observed nonlinear diffusion models using the Metropolis-Hastings algorithm. *Biometrika* **88**(3), 603–621.
- Rogers, L. C. G. and Williams, D. (2000). *Diffusions, Markov processes, and martingales. Vol. 2*. Cambridge Mathematical Library. Cambridge University Press, Cambridge. Itô calculus, Reprint of the second (1994) edition.
- Särkkä, S. (2013). *Bayesian Filtering and Smoothing*. Cambridge University Press, New York, NY, USA.
- Särkkä, S. and Sarmavuori, J. (2013). Gaussian filtering and smoothing for continuous-discrete dynamic systems. *Signal Processing* **93**(2), 500 – 510.
- Särkkä, S. and Sottinen, T. (2008). Application of Girsanov theorem to particle filtering of discretely observed continuous-time non-linear systems. *Bayesian Anal.* **3**(3), 555–584.
- Schauer, M. and contributors (2017). Bridge 0.7. *Zenodo* (10.5281/zenodo.1100978).
- Schauer, M., van der Meulen, F. and van Zanten, H. (2017). Guided proposals for simulating multi-dimensional diffusion bridges. *Bernoulli* **23**(4A), 2917–2950.
- van der Meulen, F. and Schauer, M. (2017a). Bayesian estimation of discretely observed multi-dimensional diffusion processes using guided proposals. *Electron. J. Stat.* **11**(1), 2358–2396.
- van der Meulen, F. and Schauer, M. (2017b). Bayesian estimation of incompletely observed diffusions. *Stochastics* **0**(0), 1–22.
- van der Meulen, F. and Schauer, M. (2017c). On residual and guided proposals for diffusion bridge simulation. *arXiv:1708.04870* .
- Whitaker, G. A., Golightly, A., Boys, R. J. and Sherlock, C. (2017). Improved bridge constructs for stochastic differential equations. *Statistics and Computing* **27**(4), 885–900.